Materials Science and Engineering B 176 (2011) 1028–1031

Contents lists available at ScienceDirect

Materials Science and Engineering B

journal homepage: www.elsevier.com/locate/mseb

Short communication

Enhanced light extraction from GaN-based LEDs with a bottom-up assembled photonic crystal

Haibo Gong[a,b], Xiaopeng Hao[a,*], Yongzhong Wu[a], Bingqiang Cao[b], Wei Xia[c], Xiangang Xu[a,c,*]

[a] State Key Lab of Crystal Materials, Shandong University, Jinan, 250100, PR China
[b] School of Materials Science and Engineering, University of Jinan, Jinan, 250022, PR China
[c] Shandong Huaguang Optoelectronics Company, Ltd., Jinan, 250101, PR China

ARTICLE INFO

Article history:
Received 14 January 2011
Received in revised form 27 March 2011
Accepted 2 May 2011

Keywords:
Photonic crystal
Light-emitting diode
ITO
Polystyrene sphere
Template

ABSTRACT

Photonic crystal (PhC) structure is an efficient tool for light extraction from light-emitting diodes (LEDs). The fabrication of a large area PhC structure on the light output surface of LEDs often involves sophisticated equipments such as nanoimprint lithography machine. In this study a monolayer of polystyrene (PS) microspheres was employed as a template to fabricate a noninvasive photonic crystal of indium tin oxide (ITO) on the surface of GaN-based LED. PS spheres can help to form periodic arrangement of bowl-like holes, a photonic crystal with gradually changed fill factors. Importantly, the electroluminescence intensity of LED with a photonic crystal was significantly enhanced by 1.5 times compared to that of the conventional one under various forward injection currents.

1. Introduction

Light emitting diodes (LEDs), in particular III-nitride LEDs, have progressed from being low-power indicators to high-power light sources since their invention [1]. High-brightness GaN-based LEDs yield many potential applications in outdoor display, automotive forward lighting, and backlighting of liquid crystal display, even solid-state lighting as an "ultimate lamp" in the near future [2]. However, the low light-extraction efficiency is the bottleneck for high-power LEDs. For a GaN-based standard LED, the efficiency is limited to several percents by a low light extraction efficiency due to the total internal reflection (TIR) at GaN ($n_{GaN} \sim 2.5$) and air ($n_{air} \sim 1$) boundaries [3–6].

To further harvest the generated light trapped within the GaN, many methods have been proposed to solve this problem [7], including the deposition of p-contact layers with high transmittance [8], the use of patterned sapphire substrates [9] and texturing the surface of the LEDs [10,11]. Generally, surface texturing can be obtained by e-beam lithography, nanoimprint lithography [12,13] and colloidal lithography [14–17]. For the consideration of mass production and cost effect, colloidal lithography appears to be the most efficient approach [18]. However, in the process of colloidal lithography, reactive ion etching (RIE) is usually performed to transfer the structure of colloidal sphere mask to a resist layer on GaN introducing etching damage. This may impair the active InGaN quantum wells or create defects and carrier traps on the top GaN layer and reduce the overall efficiency of the LEDs.

Our study presents a simple and effective strategy to fabricate noninvasive photonic crystals (PhCs) on GaN-based LEDs using PS spheres as templates by a bottom-up method. PS spheres can help to form a large area of photonic crystal with gradually changed fill factors. This technique can avoid the drawbacks of complicated process, sophisticated machine and etching damage and be applicable to mass production. Moreover, there is a great increase of electroluminescence of GaN-based PhC LEDs compared with conventional LEDs due to the unique diffraction properties of a photonic crystal.

2. Experimental

The GaN-based epilayer structures used in this work were grown on a *c*-plane sapphire substrate in a metal–organic chemical vapor deposition (MOCVD) system. The source gases of growing epilayers include trimethyl gallium (TMGa), triethyl indium (TEIn) and ammonia (NH_3). Hydrogen and nitrogen were used as carrier gases. Silane and dimethyl magnesium were adopted as dopants to growth n-type and p-type GaN. A sapphire substrate was heated to 1055 °C in a hydrogen flux and the substrate temperature was then lowered to 520 °C to grow the GaN nucleation buffer layer with a thickness of about 35 nm. The 1-μm-thick unintentionally doped GaN layer and the 2-μm-thick Si-doped n-type GaN film have been sequentially grown at a temperature of 1055 °C and a pressure

* Corresponding authors at: 27# Shanda South Road, Jinan, 250100, Shandong Province, PR China. Tel.: +86 531 88366218; fax: +86 531 88574135.
E-mail addresses: xphao@sdu.edu.cn, hbgong@icm.sdu.edu.cn (X. Hao).

0921-5107/$ – see front matter © 2011 Elsevier B.V. All rights reserved.
doi:10.1016/j.mseb.2011.05.026

of 500 Torr. The five-period InGaN/GaN multiple quantum wells (MQWs) structures have been grown at a temperature of 720 °C at 200 Torr. The active layer consisted of interlacedly arranged 30 Å thick InGaN-well layers and 70 Å thick GaN-barrier layers for the InGaN/GaN MQW structures. Subsequently, the Mg-doped p-type GaN films, with a thickness of 0.25 μm, were grown at a temperature of 1020 °C and a pressure of 200 Torr. The epitaxial wafer has been processed by a rapid thermal annealing at 550 °C under N_2 atmosphere to activate the doped Mg in p-GaN. Then, a 260 nm thick ITO film was deposited on the wafer by e-beam evaporation. This structure was used to fabricate the conventional LED as a reference.

Ordinary glass substrates were washed in piranha solution (98% H_2SO_4:H_2O_2 = 3:1) at 80 °C for 1 h, and then cleaned with distilled water. The PS sphere suspensions with a concentration of 2.5 wt.% were bought from Alfa Aesar Corporation. A large-area ordered colloidal monolayer (more than 10 cm^2) was deposited on glass substrates by spin coating methods. 0.2 M $SnCl_4$ and $InCl_3$ mixed solution were prepared from $SnCl_4 \cdot 5H_2O$ and $InCl_3 \cdot 4H_2O$ dissolved in distilled water (molar ratio of Sn^{4+} and In^{3+} is 1:9). The substrate with the colloidal monolayer was placed in above solution at an angle. The colloidal monolayer was then lifted off the glass substrate and floated onto the surface of the solution. Then, the floating colloidal monolayer was picked up with an epitaxial wafer with 260 nm ITO film on it (as depicted above), followed by drying at 80 °C for 1 h in an oven. Subsequently, the temperature was increased to 500 °C at a rate of 6 °C min^{-1}, and the samples were kept at 500 °C for 30 min. The morphology was examined on a field-emission scanning electron microscope.

We employed conventional photolithography to define a mesa area on the ITO-PhC structure previously coated with photoresist and on the reference structure. Two samples were etched to p-GaN layer with HCl solution to remove ITO, then followed by inductively coupled plasma (ICP) dry etching, using a BCl_3/Cl_2 mixture (constant flow rates: 10/80 sccm respectively), to transfer the mesa pattern onto the GaN layer until the n-GaN was exposed. Finally, films of metals Cr/Au (50 nm/200 nm) were evaporated using an e-beam gun to serve as p- and n-pads.

3. Results and discussion

3.1. Fabrication process of photonic crystal LEDs

PS spheres (diameter ~1 μm) were deposited on a cleaned glass substrate by spin coating method. First, the PS spheres may not be closely packed. When the glass substrate with the colloidal monolayer was placed in mixed solution of $InCl_3$ and $SnCl_4$ at an angle, the colloidal monolayer would be lifted off the glass substrate and floated onto the surface of the mixed solution on the effect of surface tension. In the lift-off process, originally dispersed microspheres shifted to each other to form closely packed monolayer. The following fabrication process of PhC LED was depicted in Fig. 1. The lifted-off PS layer was picked up by a GaN-LED wafer coated by an ITO layer deposited by e-beam evaporation. The pre-deposited ITO layer on the GaN epitaxial wafer was more compact than the final formed PhC-ITO. So the compact ITO layer with lower resistance can act as an efficient current-spreading layer. For comparison purpose,

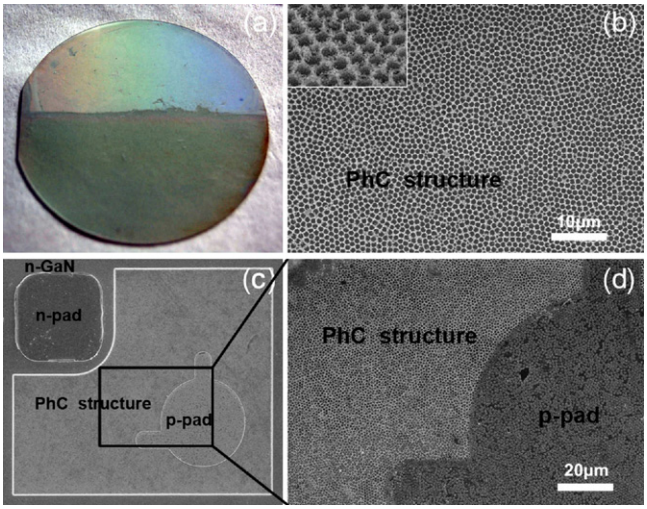

Fig. 2. (a) A photograph of GaN-based wafer with the upper half covered by a monolayer of PS microspheres. (b) SEM image of the photonic crystal structure after calcinations (the inset in top left corner showed the tilted view of PhC). (c) SEM image of a PhC GaN-based LED (11 mil × 13 mil). (d) Topography of partial p-pad and light extraction zone of a PhC LED as indicated in square of (c).

only one half of the wafer was covered by PS microspheres layer as shown in Fig. 2a. The wafer with PS spheres and ITO solution was dried and calcinated at atmosphere. During the calcination, $InCl_3$ and $SnCl_4$ reacted with oxygen to form In_2O_3 and SnO_2 while PS spheres were decomposed to turn into CO_2. ITO film is considered to be a high performance semiconductor oxide and being widely used in liquid crystal display and related area. The doping of Sn in In_2O_3 can help to form high-quality ITO film with high transmittance and conductivity. The commonly used ITO film (molar ratio of Sn/In is 1/9) has the best conductivity and a high transmittance (above 90%). So, in our work, the content of Sn is 10% with respect to the total amount of In and Sn and the formed ITO photonic crystal can further act as transparent current spreading layer.

3.2. Surface morphology of photonic crystal LEDs

Fig. 2b shows the surface morphology of the wafer after calcination. The bowl-like air holes were nearly hexagonally close arranged with an opening diameter of about 1 μm and the maximal depth of the holes is 500 nm (the radius of a PS sphere). As last step, the LED chip was fabricated conventionally and its electronic performance was tested. Fig. 2c presents a photograph of a PhC-LED chip. The square on the top left corner of the chip is n-pad and the p-pad is on the down right. To identify the texture of the PhC-LED light-emitting area, a part of the chip surface including p-pad and light-extraction region was zoomed in as indicated in Fig. 2d.

3.3. Electroluminescence analysis of LED devices

Fig. 3a shows the voltage–current–luminance characteristics of the LEDs with and without photonic crystal. With the increase of injection current, the luminance intensity of emitted light boosted to a higher level, to 118 mcd and 177 mcd at 80 mA for conventional

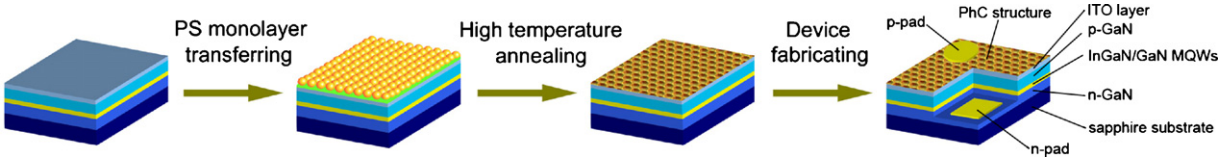

Fig. 1. The fabricating process of photonic crystal LED using a monolayer of PS spheres as a template.

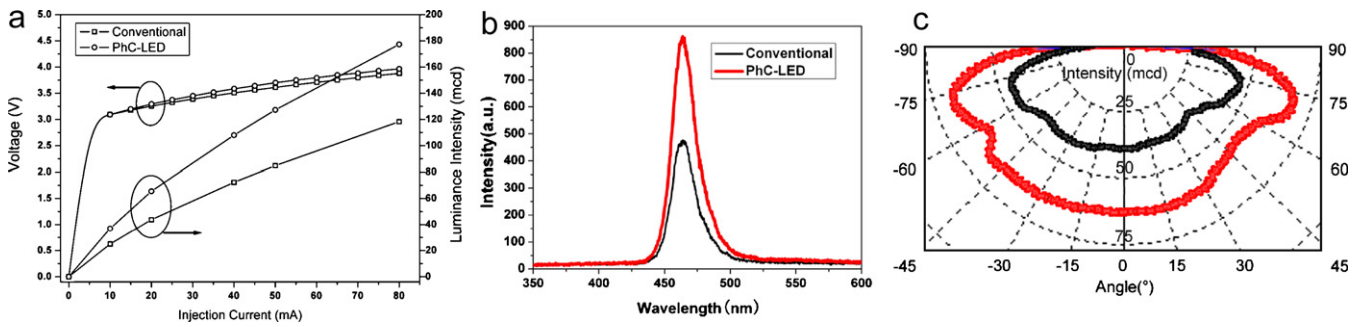

Fig. 3. (a) A plot of voltage–current–luminance intensity characteristics of fabricated LEDs with and without PhC. (b) Electroluminescence spectra and (c) Angular distributions of far-field radiations from an unencapsulated PhC-LED (red bold curve) and a conventional LED (black thin curve) at an injection current of 20 mA. (For interpretation of the references to color in this figure legend, the reader is referred to the web version of the article.)

and PhC LED respectively. At a commonly used testing injection current of 20 mA, the output intensity of the LED without photonic crystals was 44 mcd and with PhC-LED 65 mcd. So the corresponding output luminance intensity enhancements were about 50% at both 20 mA and 80 mA. The forward voltage for the PhC-LED (3.21 V at 20 mA) was nearly identical to that of the conventional LED without photonic crystals (3.20 V at 20 mA). The peak emission wavelengths of the LEDs with and without photonic crystal were 466 nm As displayed in Fig. 3b and peak intensity of PhC-LED was about 1.7 times as high as the conventional, which is nearly consistent with the value as shown in Fig. 3a. In addition, the far-field radiation angular distributions of the PhC-LEDs and normal LEDs were also measured from −90° to 90° at an injection current of 20 mA (shown in Fig. 3c). There were not obvious differences in shape between the two LEDs' radiation patterns. This is contradictory to the result reported by Ryu and co-workers [19]. The reason may be that, in contrast with the so-called bandgap approach, the diffractive properties of PhCs dominated here, due to the relatively large lattice constant compared with the light wavelength. However, the intensities of emitted lights from the PhC-LED in nearly every angle is 1.5 times as strong as the conventional LED and this result is consistent with their current–luminance characteristics as indicated in Fig. 3a at 20 mA.

In a conventional GaN-LED most of the emitted light is trapped in the GaN layer by TIR at the air/GaN interfaces. This light is labeled as guided light and the integrated PhC only aims at extracting this guided light. Each of the guided modes can be characterized by an in-plane wavevector $k_{\|m}$ (parallel to the surface of the LED). IF k_0 is the in-plane wave vector in air, modes below the light line ($|k_{\|m}| > |k_0|$) suffer TIR and cannot phase match to the radiation modes. Phase matching requires that $k_0 = k_{\|m} \pm G$, where G is a reciprocal lattice vector of a photonic crystal. The photonic crystal, however, folds the guided modes at the Brillouin zone boundaries, allowing phase matching to the radiation modes that lie above the air light line [20]. The guided modes that phase match to radiation modes become leaky resonances of the photonic crystal. Thus, the photonic crystal Bragg scatters emitted light out of the semiconductor as a diffraction grating, leading to higher extraction efficiencies.

However, as reported by David et al. [21], using shallow PhCs on top of a GaN layer, diffraction of guided modes could not be observed. This was attributed to their poor overlap with the PhC. One could therefore consider deeper PhC in order to increase the interaction between the PhC and these guided modes. However, as the average refractive index in the PhC region (typically <2) is smaller than the effective index of the low-order modes, guided modes are strongly evanescent in the holes region so that their diffraction does not increase significantly for a PhC depth larger than λ/n. The depth of our fabricated PhC is large enough to effectively enhance the light extraction. Furthermore, lattice constant of PhCs should be larger than 2/3 of the wavelength for efficient light extraction as reported by Ichikawa and Baba [22]. So it can also be satisfied using 1 μm PS microspheres as templates.

It should be noticed that the common photonic crystals are composed of holes with vertical walls as previously reported. One mainly concentrates on the periods, fill factors, holes diameters, arrangements and depths. However, the effect of wall profiles on the properties of photonic crystals has not been investigated yet. In our work, the shapes of the holes are bowl-like and the fill factor is gradually changed with the depth of holes. Furthermore, as shown in Fig. 2b the holes were not completely arranged into triangular array but in quasi-period arrangement. And this may provide more reciprocal lattice vectors to match with guided modes. So the photonic crystal can support more guided modes to meet phase matching condition and the extraction efficiency should be more efficient than the conventional PhCs. Works that are ongoing include different diameters of bowl-like holes and corresponding computational simulations.

4. Conclusion

In conclusion, using a monolayer of PS microspheres as a template, we have demonstrated a simple and flexible synthesis strategy for fabricating noninvasive photonic crystals. Based on the bottom-up method, blue-light PhC LEDs were manufactured and the light extraction was enhanced by up to 50% at various injection currents.

Acknowledgements

This work was supported by the NSFC, National Basic Research Program of China (973 Program), the Fund for the Natural Science of Shandong Province, the Scientific Research Award for the Excellent Middle-Aged and Young Scientists of Shandong Province, the Doctorial Fund and Scientific Fund of UJN.

References

[1] J.J. Wierer, A. David, M.M. Megens, Nat. Photonics 3 (2009) 163–169.
[2] M. Koike, N. Shibata, H. Kato, Y. Takahashi, IEEE J. Sel. Top. Quantum Electron 8 (2002) 271–277.
[3] E.F. Schubert, J.K. Kim, Science 308 (2005) 1274–1278.
[4] M.P. Krames, O.B. Shchekin, R.M. Mach, G.O. Mueller, L. Zhou, G. Harbers, M.G. Craford, J. Disp. Technol. 3 (2007) 160–175.
[5] J.V. Smith, Geometrical and Structural Crystallography, Wiley, New York, USA, 1982, p. 449.
[6] H. Ichikawa, T. Baba, Appl. Phys. Lett. 84 (2004) 457–459.
[7] A.I. Zhmakin, Phys. Rep. 498 (2011) 189–241.
[8] S.J. Chang, C.S. Chang, Y.K. Su, R.W. Chuang, W.C. Lai, C.H. Kuo, Y.P. Hsu, Y.C. Lin, S.C. Shei, H.M. Lo, J.C. Ke, J.K. Sheu, IEEE Photonics Technol. Lett. 16 (2004) 1002–1004.
[9] C.C. Wang, H. Ku, C.C. Liu, K.K. Chong, C.I. Hung, Y.H. Wang, M.P. Houng, Appl. Phys. Lett. 91 (2007) 1–3, 121109.

[10] T. Fujii, Y. Gao, R. Sharma, E.L. Hu, S.P. DenBaars, S. Nakamura, Appl. Phys. Lett. 84 (2004) 855–857.
[11] C.H. Kuo, H.C. Feng, C.W. Kuo, C.M. Chen, L.W. Wu, G.C. Chi, Appl. Phys. Lett. 90 (2007) 1–3, 142115.
[12] S.J. Chang, C.F. Shen, W.S. Chen, C.T. Kuo, T.K. Ko, S.C. Shei, J.K. Sheu, Appl. Phys. Lett. 91 (2007) 13504–13506.
[13] T.A. Truong, L.M. Campos, E. Matioli, I. Meinel, C.J. Hawker, C. Weisbuch, P.M. Petroff, Appl. Phys. Lett. 94 (2009) 1–3, 23101.
[14] R.H. Horng, C.C. Yang, J.Y. Wu, S.H. Huang, C.E. Lee, D.S. Wu, Appl. Phys. Lett. 86 (2005) 1–3, 221101.
[15] Y.K. Su, J.J. Chen, C.L. Lin, S.M. Chen, W.L. Li, C.C. Kao, Jpn. J. Appl. Phys. 47 (2008) 6706–6708.
[16] C.H. Chan, C.H. Hou, C.K. Huang, T.J. Chen, S.Z. Tseng, H.T. Chien, C.H. Kuo, K.H. Hsieh, Y.L. Tsai, K.C. Hsu, C.C. Chen, Jpn. J. Appl. Phys. 48 (2009) 20212–20214, Part 1.
[17] M.Y. Hsieh, C.Y. Wang, L.Y. Chen, T.P. Lin, M.Y. Ke, Y.W. Cheng, Y.C. Yu, C.P. Chen, D.M. Yeh, C.F. Lu, C.F. Huang, C.C. Yang, J.J. Huang, IEEE Electron Device Lett. 29 (2008) 658–660.
[18] C.H. Hou, S.Z. Tseng, C.H. Chan, T.J. Chen, H.T. Chien, F.L. Hsiao, H.K. Chiu, C.C. Lee, Y.L. Tsai, C.C. Chen, Appl. Phys. Lett. 95 (2009) 133105–133107.
[19] J. Park, J.K. Oh, K.W. Kwon, Y.H. Kim, S.S. Jo, J.K. Lee, S.W. Ryu, IEEE Photonics Technol. Lett. 20 (2008) 321–323.
[20] V.N. Astratov, I.S. Culashaw, R.M. Stevenson, D.M. Whittaker, M.S. Skolnick, T.F. Krauss, R.M. De La Rue, J. Lightwave Technol. 17 (1999) 2050–2057.
[21] A. David, T. Fujii, R. Sharma, K. McGroddy, S. Nakamura, S.P. DenBaars, E.L. Hu, C. Weisbuch, H. Benisty, Appl. Phys. Lett. 88 (2006) 61124–61126.
[22] H.W. Huang, J.T. Chu, C.C. Kao, T.H. Hseuh, T.C. Lu, H.C. Kuo, S.C. Wang, C.C. Yu, Nanotechnology 16 (2005) 1844–1848.